Supplementary Information

Adaptive multiscale microscope with fast zooming, extended working distance, and large field of view

Yi Zheng[1], Xin Wang[1], Zhao Jiang[1], Jin-Bo Xu[1], Rong-Ying Yuan[1], You-Ran Zhao[1], Hao-Ran Zhang[1], Chao Liu[1,2 *], Qiong-Hua Wang[1,2 *]

[1] School of Instrumentation and Optoelectronic Engineering, Beihang University, Beijing 100191, China.

[2] State Key Laboratory of Virtual Reality Technology and Systems, Beihang University, Beijing 100191, China.

*Correspondence: C. Liu, E-mail: chaoliu@buaa.edu.cn; Q. H. Wang, E-mail: qionghua@buaa.edu.cn

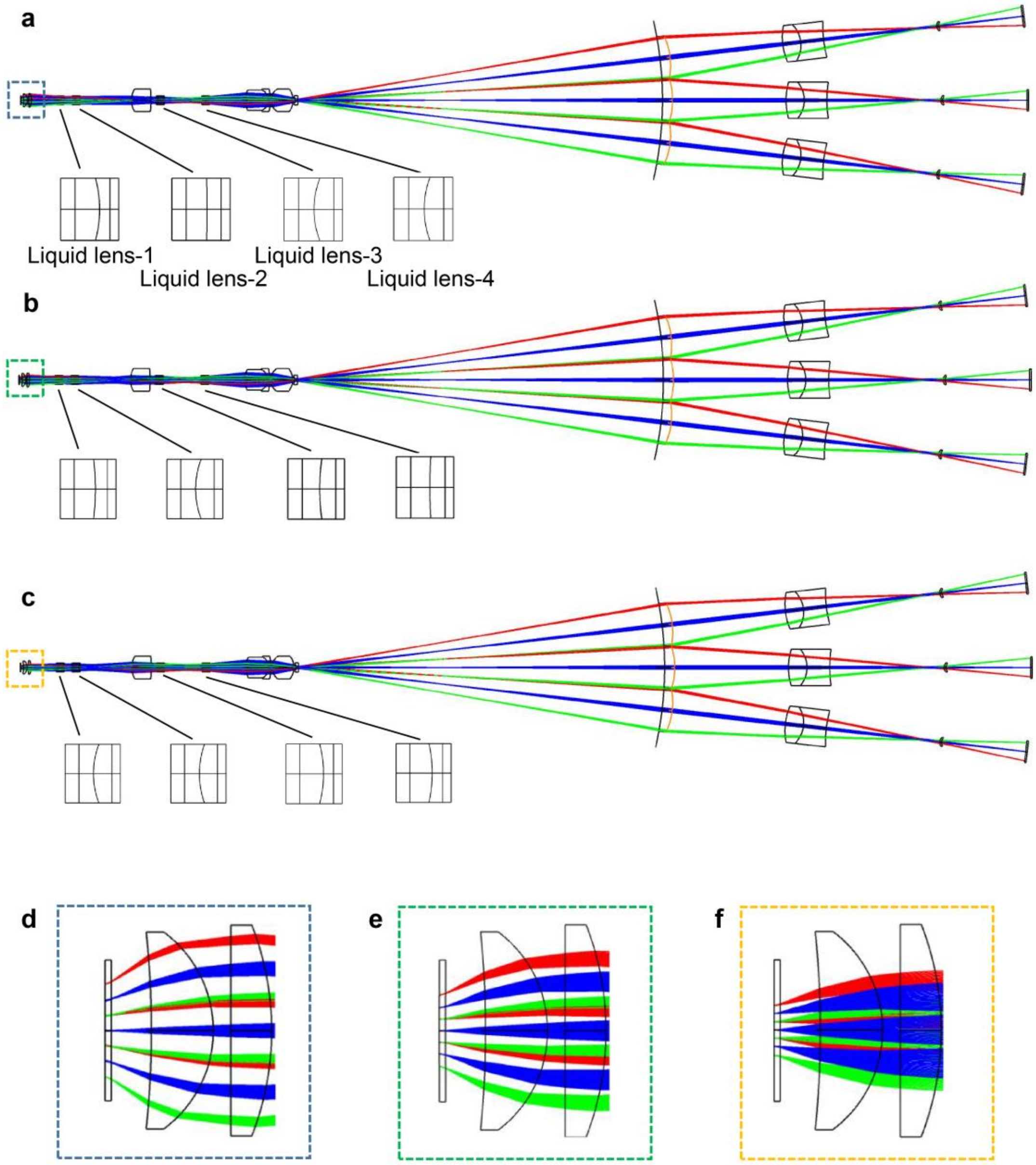

Supplementary Figure S1 Optical path simulation of the proposed microscope. a–c Simulated optical path of the microscope at magnifications of 9×, 13×, and 18×. **d–f** Local enlarged images of the simulated optical path at magnifications of 9×, 13×, and 18×.

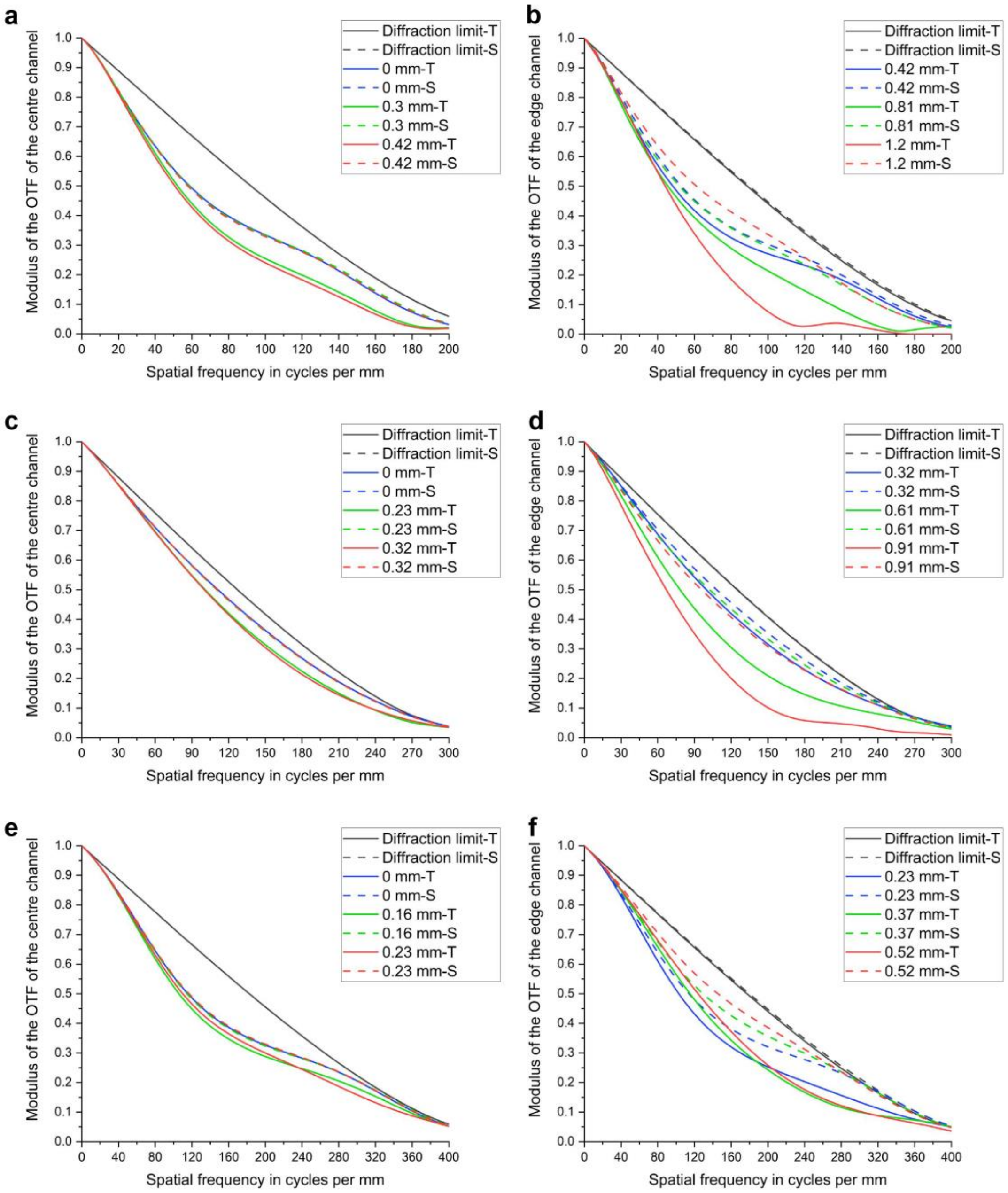

Supplementary Figure S2 Simulation of modulus of the optical transfer function (OTF) at different object heights and magnifications. a, b Modulus of the OTF at different object heights and magnification of 9× in the centre and edge channels. **c, d** Modulus of the OTF at different object heights and magnification of 13× in the centre and edge channels. **e, f** Modulus of the OTF at different object heights and magnification of 18× in the centre and edge channels. (T and S represent tangential plane and sagittal plane, respectively. 0 mm, 0.3 mm, etc are object heights.)

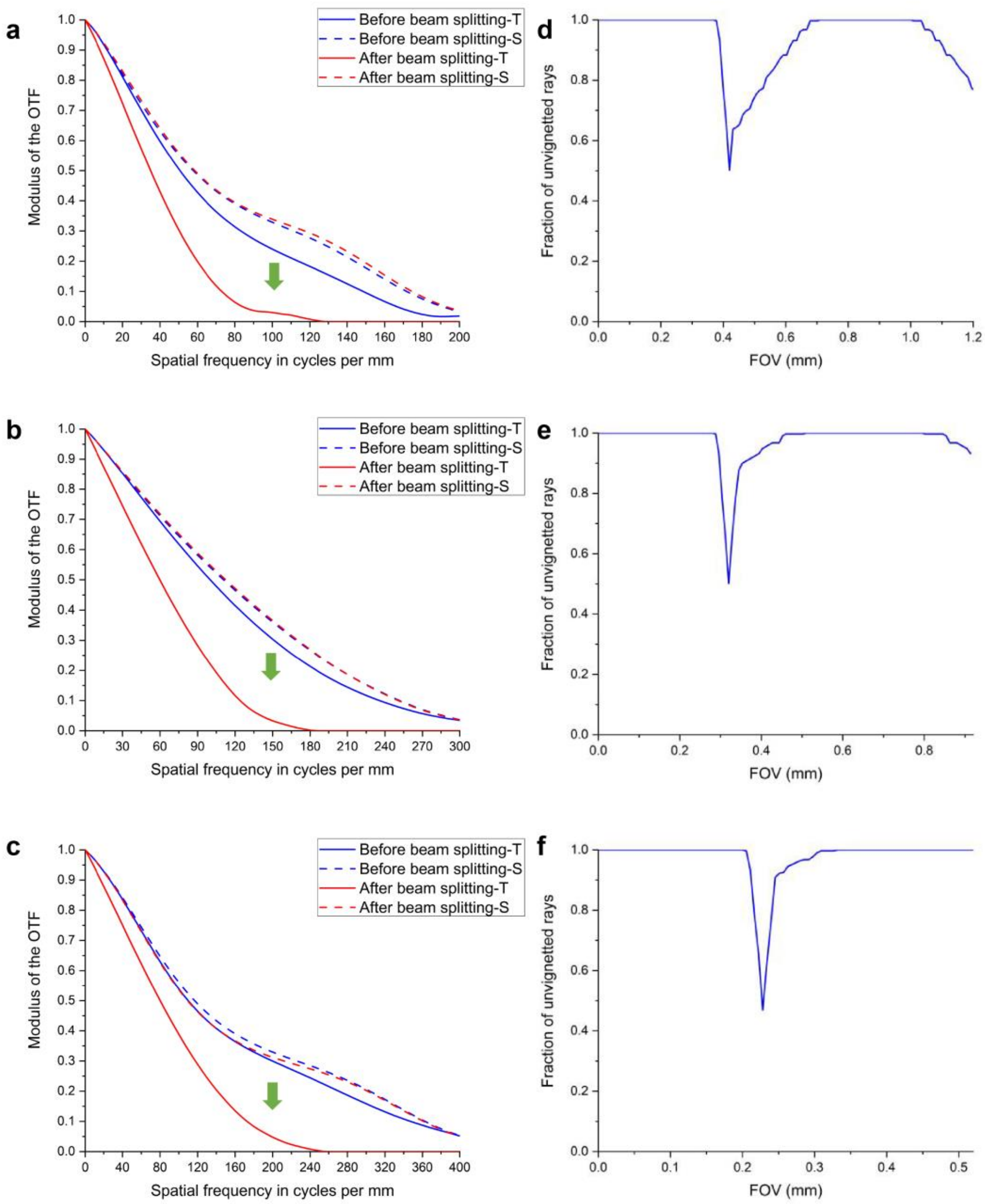

Supplementary Figure S3 Reduction in resolution and illumination due to spectroscopic effects. a–c Simulated resolution reduction at the field-of-view (FOV) intersection of centre and edge channels at magnifications of 9×, 13×, and 18×. **d–f** Simulated fraction of unvignetted rays at different FOVs (or object heights) with magnifications of 9×, 13×, and 18×.

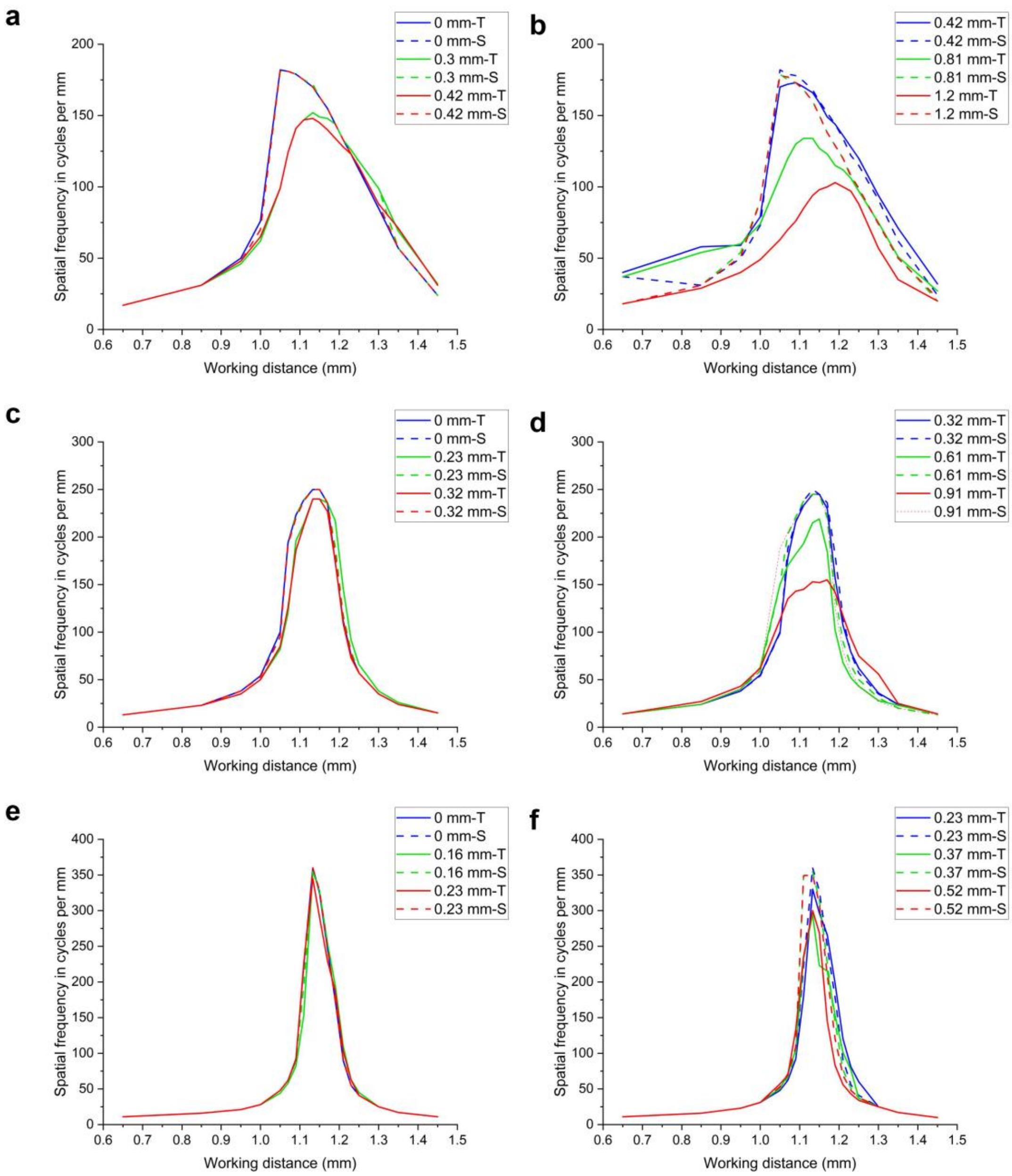

Supplementary Figure S4 Depth of fields at different magnifications. a, b Corresponding spatial frequency curves when the modulus of the OTF is 0.1 in the centre and edge channels at different working distances and magnification of 9×. **c, d** Corresponding spatial frequency curves when the modulus of the OTF is 0.1 in the centre and edge channels at different working distances and magnification of 13×. **e, f** Corresponding spatial frequency curves when the modulus of the OTF is 0.1 in the centre and edge channels at different working distances and magnification of 18×.

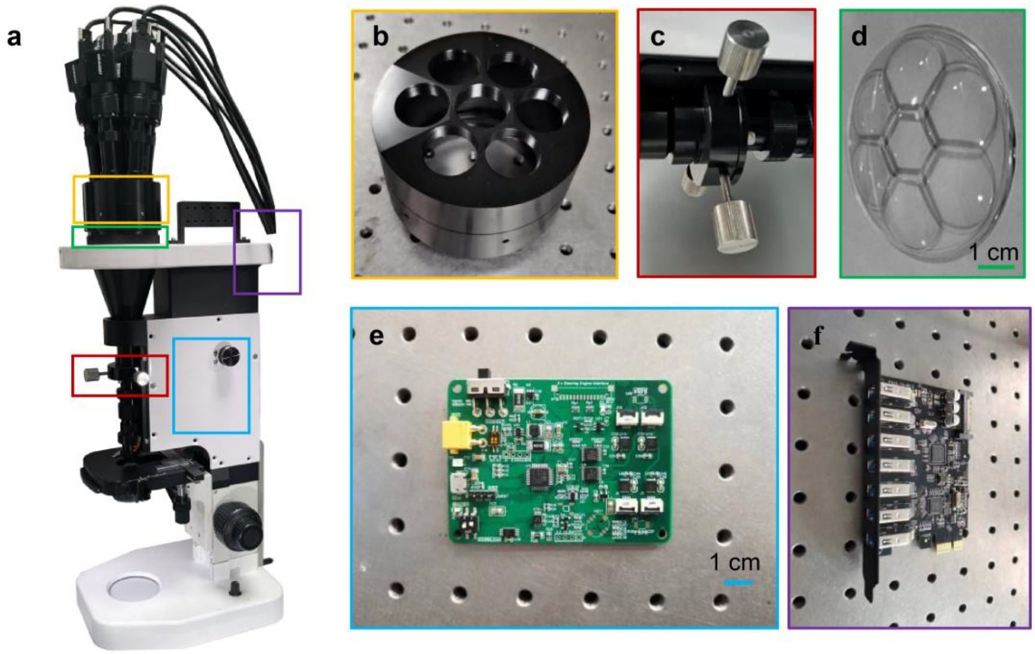

Supplementary Figure S5 Fabrication of the proposed microscope. a Real image of the proposed microscope. **b, c** Real images of the assembly and adjustment mechanisms. **d** Real image of the compound eye lens. **e** Real image of the liquid lens driver. **f** Real image of the seven-channel data stream transmission port.

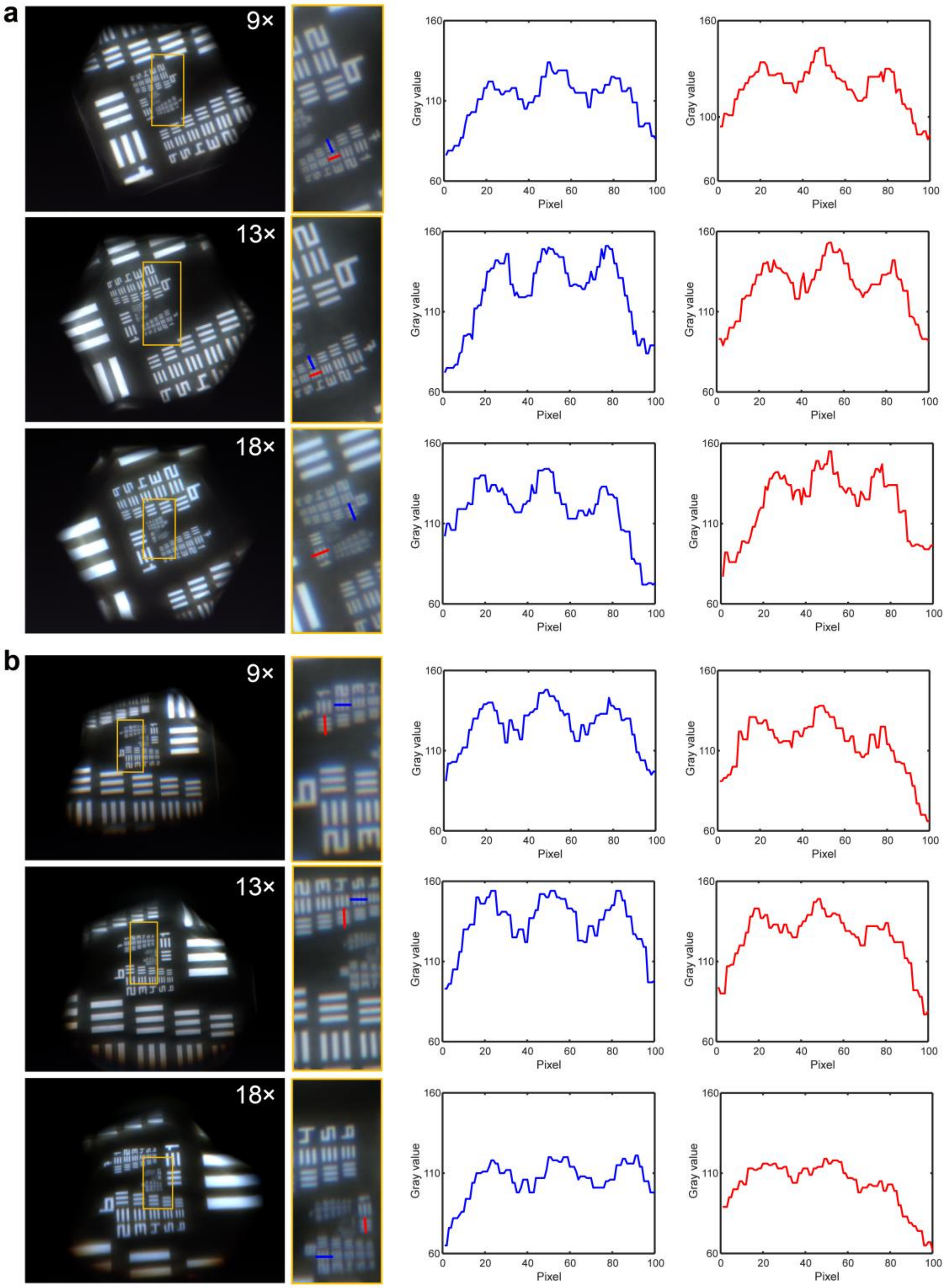

Supplementary Figure S6 Resolution test at different magnifications. a Resolution test results of the centre channel at magnifications of 9×, 13×, and 18×. **b** Resolution test results of the edge channel at magnifications of 9×, 13×, and 18×.

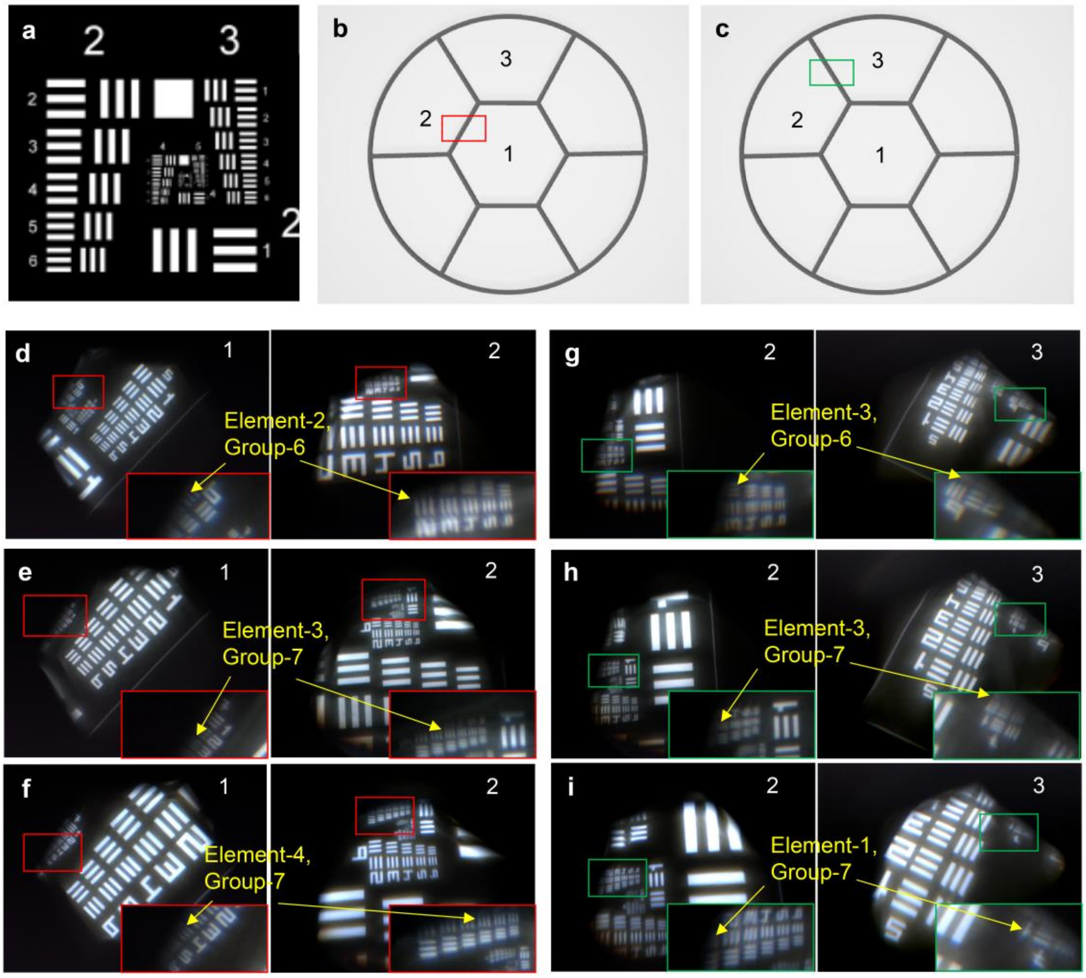

Supplementary Figure S7 Verification experiments of FOV overlapping. a Image of the resolution test target. **b** Schematic diagram of placing the resolution test target in the boundary area between FOV #1 and #2. **c** Schematic diagram of placing the resolution test target in the boundary area between FOV #2 and #3. **d–f** Captured images of FOV #1 and #2 when placing the resolution test target in the boundary area between FOV #1 and #2 at magnifications of 9×, 13×, and 18×. **g–i** Captured images of FOV #2 and #3 when placing the resolution test target in the boundary area between FOV #2 and #3 at magnifications of 9×, 13×, and 18×.

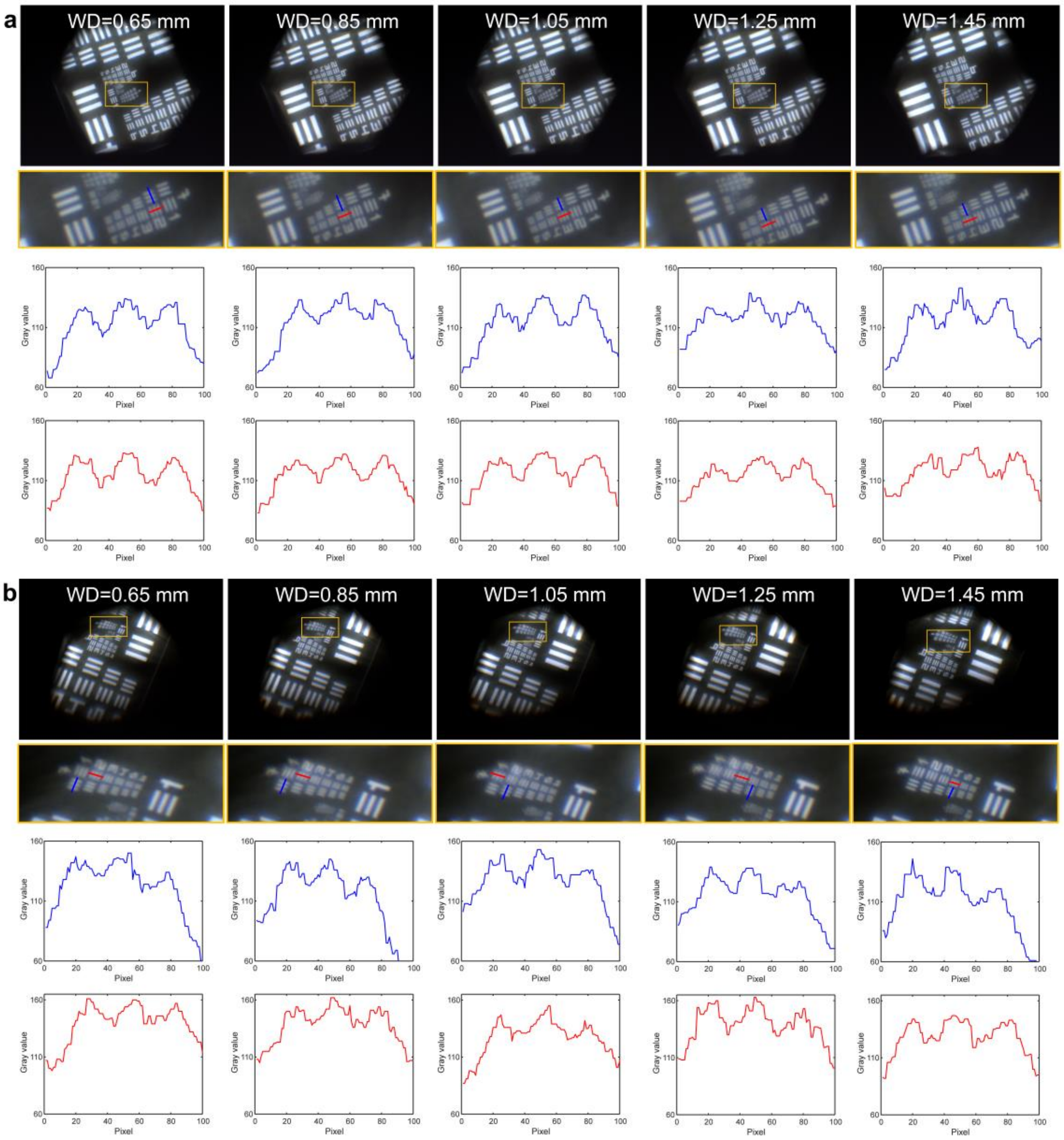

Supplementary Figure S8 Resolution test with different working distances (WDs) at initial magnification of 9×. a Resolution test results of the centre channel with different WDs at initial magnification of 9×. **b** Resolution test results of the edge channel with different WDs at initial magnification of 9×.

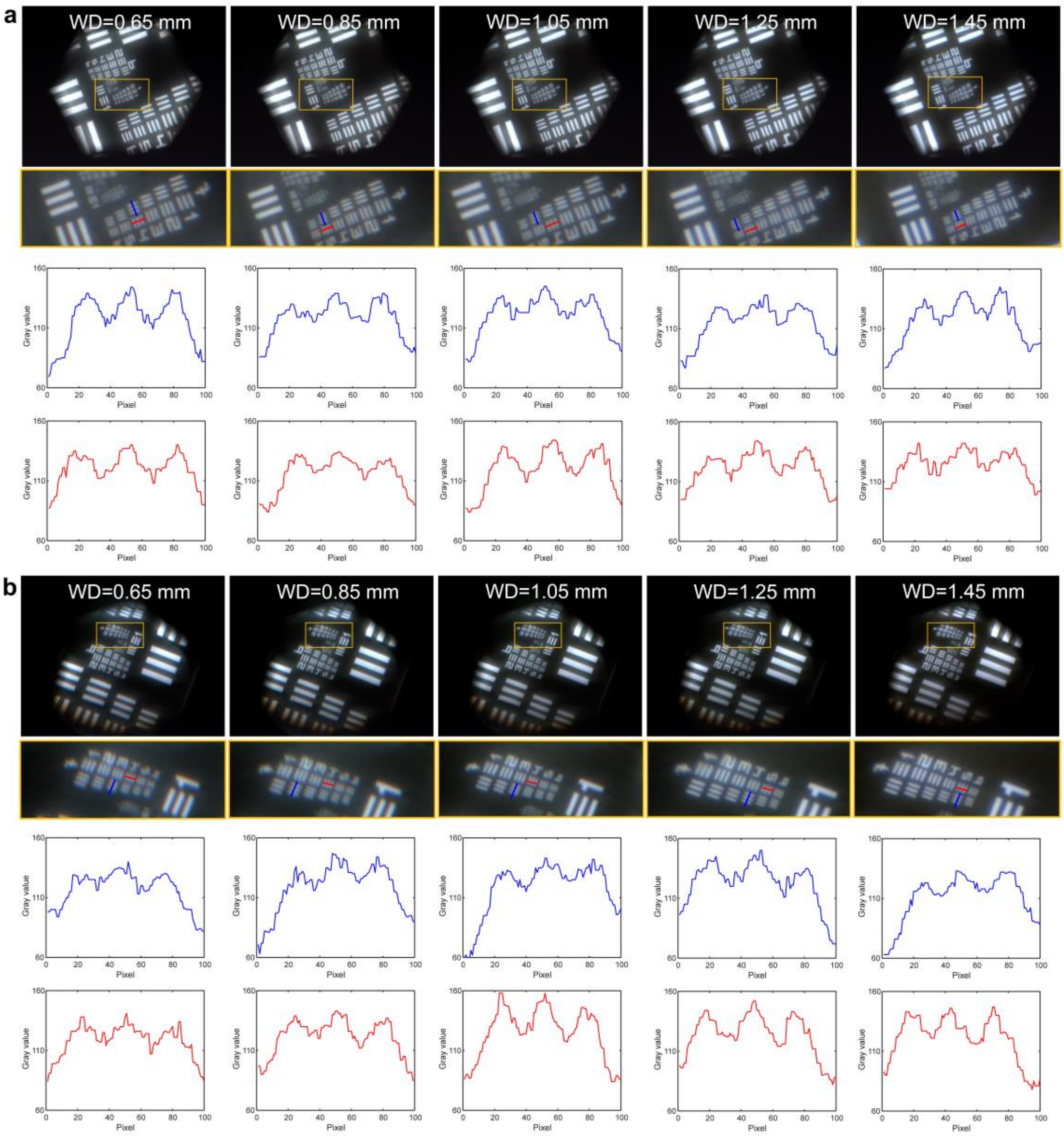

Supplementary Figure S9 Resolution test with different working distances (WDs) at initial magnification of 13×. a Resolution test results of the centre channel with different WDs at initial magnification of 13×. **b** Resolution test results of the edge channel with different WDs at initial magnification of 13×.

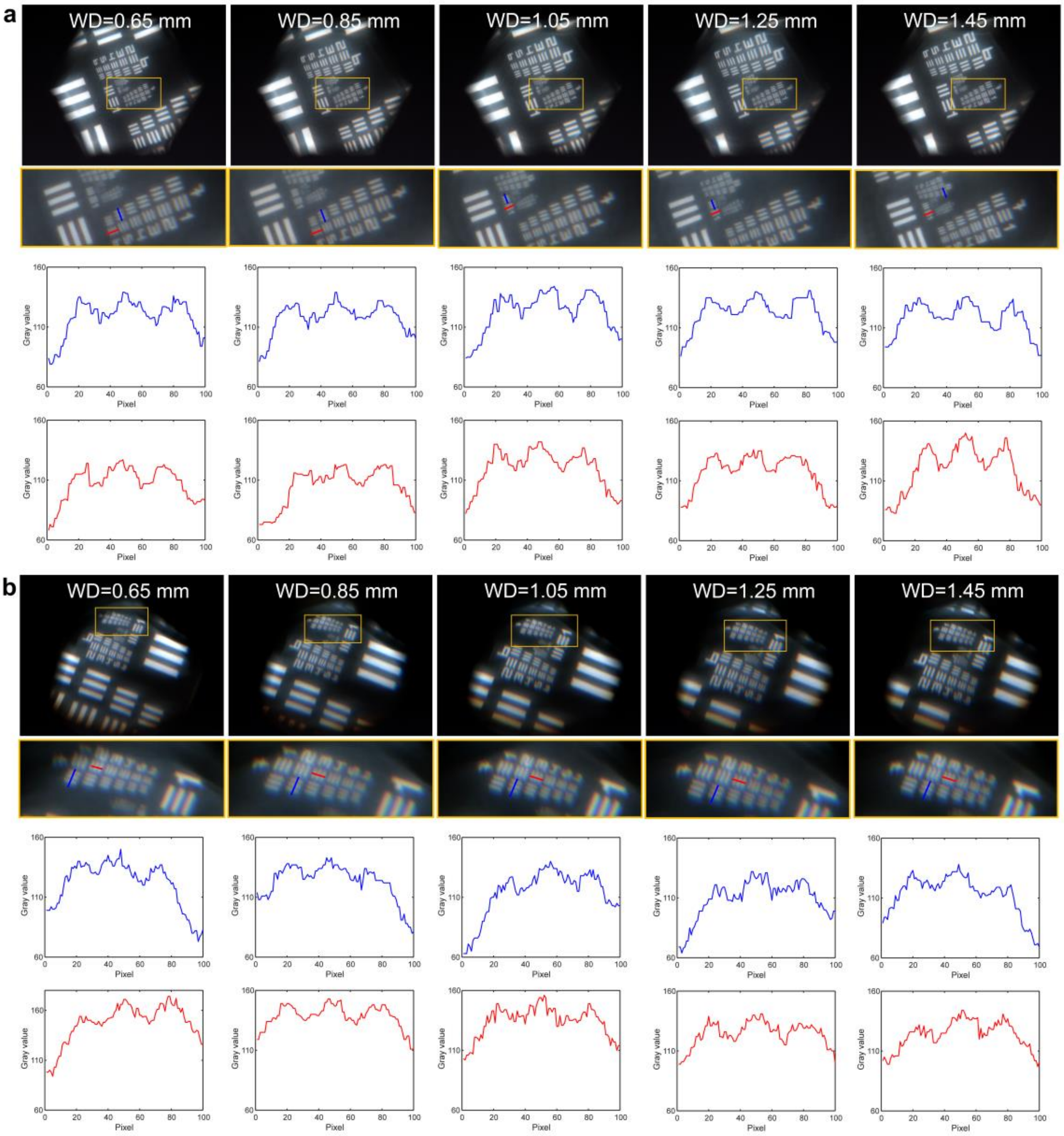

Supplementary Figure S10 Resolution test with different working distances (WDs) at initial magnification of 18×. a Resolution test results of the centre channel with different WDs at initial magnification of 18×. **b** Resolution test results of the edge channel with different WDs at initial magnification of 18×.

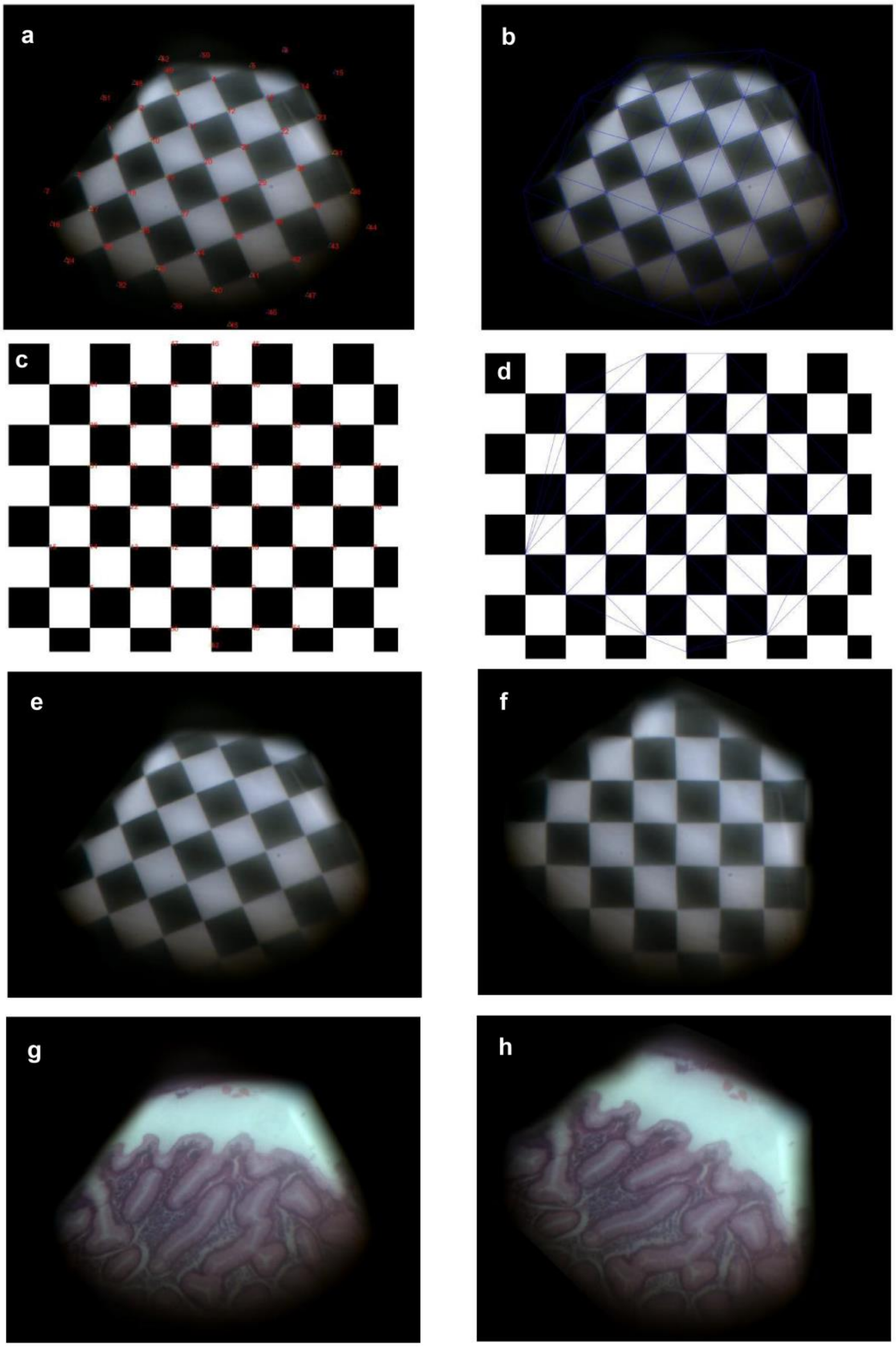

Supplementary Figure S11 Distortion correction by the nonuniform-distortion-correction algorithm. a Chequerboard image vertex markers. **b** Triangle area division of chequerboard image. **c** Correspondence between the marked vertices in the image and the vertices of the standard chequerboard. **d** Correspondence between the marked triangle area in the image and the standard chequerboard triangle area. **e, f** Chequerboard images before and after distortion correction. **g, h** Sample images before and after distortion correction.

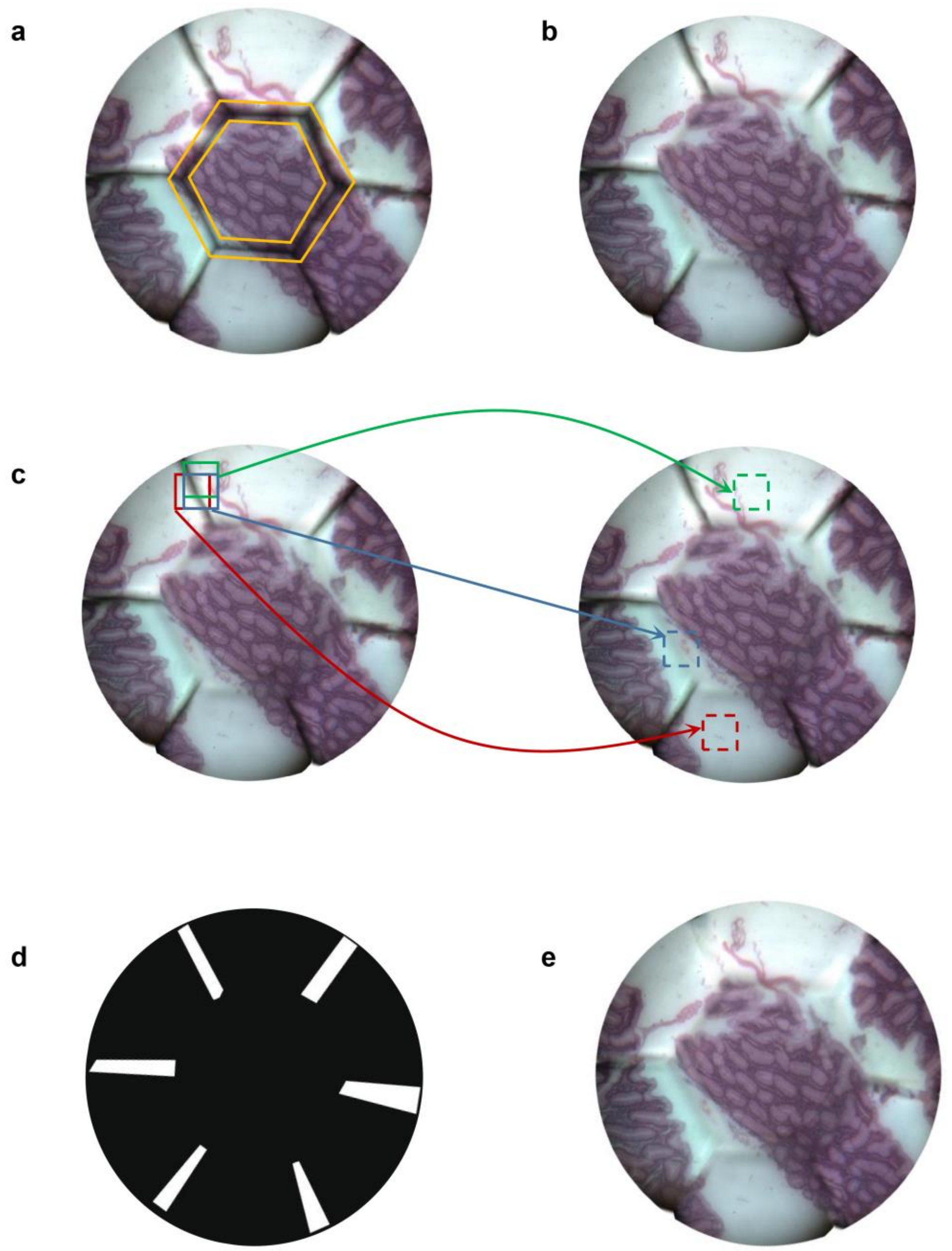

Supplementary Figure S12 Vignetting processing by the composite patching algorithm. a Image after distortion correction at magnification of 13×. **b** Image obtained by filling the pixels at the edge of the centre FOV image at magnification of 9× into the orange area in Supplementary Fig. S12a. **c** Initialization offset process of patching the vignetted boundary around the edge FOVs using PatchMatch algorithm. **d** Mask image for marking the area to be filled around the edge FOVs. **e** Final image after vignetted boundary processing.

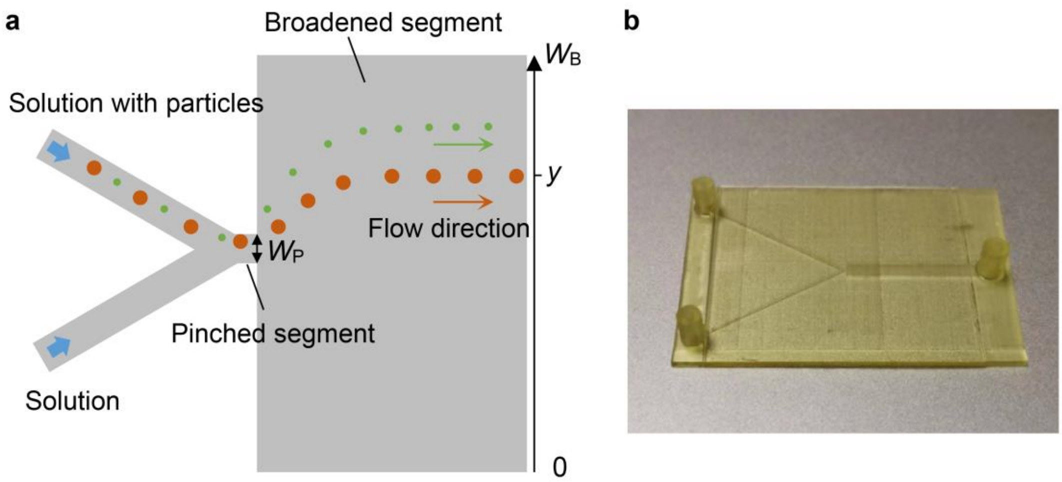

Supplementary Figure S13 Principle and structure of the microfluidic chip for separation of particles. **a** Principle of the microfluidic chip for separation of particles. **b** Real image of the microfluidic chip.

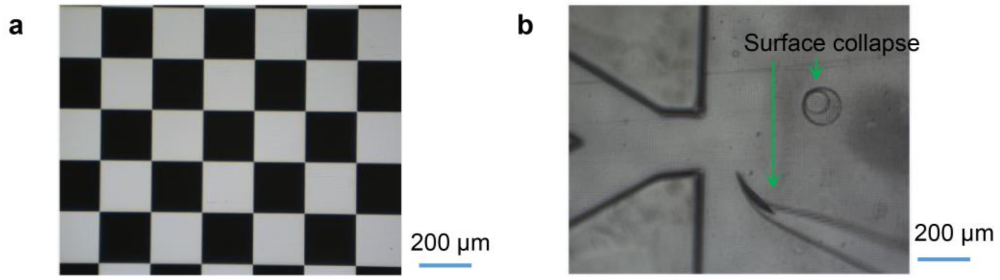

Supplementary Figure S14 FOV of an ordinary microscope. a Chequerboard image captured by the commercial microscope with 10× objective lens. **b** Microfluidic chip image captured by the commercial microscope.